A modelling study of Norway lobster (*Nephrops norvegicus*) larval dispersal in southern Portugal: predictions of larval wastage and self-recruitment in the Algarve stock

Martinho Marta-Almeida, Jesus Dubert, Álvaro Peliz, Antonina dos Santos, and Henrique Queiroga

Abstract: A set of simulations using a validated and realistic parameterization of a numerical model was conducted for the south and southwest Portuguese regions as an attempt to understand larval dispersal patterns in the Norway lobster (*Nephrops norvegicus*). Larvae were introduced in the model as Lagrangian particles with five different behavioural scenarios concerning their ability to migrate vertically. Growth rate was temperature dependent and the larvae were tracked individually. The end point of the simulations was the position of the larvae when they reached competency at age 1. Age 1.25 was also considered to simulate a possible delay in settling due to lack of an appropriate substrate. The results showed that the majority of the larvae reached age 1 near the hatching area along the southern shelf, while low exchange of larvae between the south and the west coasts was observed, especially for behavioural scenarios where larvae remained in relatively shallow waters. Scenarios where larvae performed diurnal vertical migration and delayed settlement until age 1.25 indicated a tendency for westward motion because of interactions with the Mediterranean undercurrent. Self-recruitment to the Algarve stock was estimated at 0.2% to 0.5%, raising the concern that this stock may be experiencing recruitment limitation.

Résumé : Nous avons réalisé une série de simulations à l'aide d'un modèle numérique doté de paramètres validés et réalistes dans les régions portugaises du sud et du sud-ouest pour tenter de comprendre les patrons de dispersion des larves chez le homard de Norvège (*Nephrops norvegicus*). Nous avons introduit les larves dans le modèle comme des particules lagrangiennes possédant différents scénarios comportementaux relatifs à leur capacité de migration verticale. Le taux de croissance est dépendant de la température et les larves ont pu être suivies individuellement. Le terme final des simulations est la position des larves au moment où elles peuvent vivre indépendamment à l'âge 1. Nous avons aussi examiné l'âge 1,25 pour simuler la possibilité de délais dans l'établissement dus à la pénurie de substrats appropriés. Les résultats montrent que la majorité des larves atteignent l'âge 1 près du lieu d'éclosion le long de la plate-forme sud; on peut cependant observer un faible échange de larves entre les côtes sud et ouest, particulièrement dans les scénarios comportementaux dans lesquels les larves demeurent en eaux relativement peu profondes. Les scénarios dans lesquels les larves font des migrations verticales diurnes et retardent leur établissement jusqu'à l'âge 1,25 montrent une tendance vers un déplacement vers l'ouest à cause des interactions avec le courant sous-marin de la Méditerranée. Nous estimons l'auto-recrutement du stock de l'Algarve à 0,2 % à 0,5 %, ce qui soulève des inquiétudes sur la possibilité de limitation du recrutement dans ce stock.

[Traduit par la Rédaction]

Introduction

The Norway lobster (*Nephrops norvegicus*) is a burrowing decapod crustacean with an extended distribution in the palearctic Atlantic and Mediterranean regions. According to the International Council for the Exploration of the Sea (ICES 2006), this species is commercially exploited throughout its geographic area, with landings around 600 t per year in the ICES area IXa (West Galicia, Portugal, and Gulf of Cadiz). The economic importance of the species has promoted considerable interest in several aspects of its biology, such as growth, reproduction, and spatial structure of

Received 29 July 2007. Accepted 24 April 2008. Published on the NRC Research Press Web site at cjfas.nrc.ca on 4 October 2008. J20113

M. Marta-Almeida,[1] J. Dubert, and H. Queiroga. Centro de Estudos do Ambiente e do Mar (CESAM), Departamento de Física, Universidade de Aveiro, Portugal.
Á. Peliz. Instituto de Oceanografia, Universidade de Lisboa, Lisboa, Portugal.
A. dos Santos. Instituto Nacional de Recursos Biológico (INRB/L-IPIMAR), Lisboa, Portugal.

[1]Corresponding author (e-mail: mma@ua.pt).

the populations (e.g., Farmer 1974; Maynou et al. 1998; Tuck et al. 2000). The species is one of the most valuable demersal shellfish resources in Portugal, where it is targeted, along with a mix of other species, by the demersal trawl fleet. Until the late 1980s, *Nephrops* was the main species captured by the trawl fleet, but catches have decreased considerably during the 1990s to minimum values in 1996 and 1997 (ICES 2006). This situation led to the implementation and enforcement of a recovery plan applied to the Iberian Atlantic stocks since 2006. While the observed catch decrease is largely caused by the fishery pressure, there is the concern that some of the variability could be due to environmental effects, particularly during the larval phase.

It is commonly accepted that oceanic currents play a major role in the retention and (or) dispersal of *Nephrops* larvae from hatching areas and in the recruitment back to settlement sites (White et al. 1988; Hill 1990; Bailey et al. 1995). In the Irish Sea, where most larvae occur between surface waters and 50 m depth (Harding and Nichols 1987; Lindley et al. 1994), larvae can be transported away from hatching areas by the density-driven circulation (White et al. 1988). Diel vertical migration (DVM) is a common behavioural pattern in decapod larvae that influences dispersal distances and pathways (Queiroga and Blanton 2004), and in the shallow North and Irish seas *Nephrops* zoeae have been reported to perform this type of migration, occurring close to the surface at night (Hillis 1974; Lindley et al. 1994). However, nothing is known about the vertical distribution of this species' larvae along the Portuguese and Mediterranean coasts, where *Nephrops* lives much deeper. Interest on the larval ecology of *Nephrops* has also been raised by several studies on genetic geographic structure (Maltagliati et al. 1998; Stamatis et al. 2004, 2006), which consistently showed small but statistically significant genetic divergence at the regional scale (10s to 100s of kilometres) but a lack of isolation-by-distance differentiation, as well as phylogenetic trees without geographical meaning, across the distributional range of the species (1000s of kilometres). Given that adults are sedentary, most of the dispersal should be accomplished during the larval phase. The lack of geographic structure at the large scale has been interpreted as resulting from post-Pleistocenic range expansion shaping the current genetic structure of *Nephrops* polulations and not by exchange of larvae among such distant regions as the North and the Aegean seas (Stamatis et al. 2004). However, the question remains open on the importance of larval exchange on demographic and genetic connectivity between populations at scales of 100s of kilometres.

Nephrops norvegicus adults are commonly found in depths ranging from 90 to 800 m along the Portuguese shelf and slope areas, on bottoms composed of sticky mud (Figueiredo and Thomas 1967). The distribution is patchy, with the largest area of high abundance located off the south coast of Portugal, in the plateau areas surrounding the Diogo Cão deep (centred at 36.67°N, 7.67°W). Egg spawning in Portugal occurs in August and September, and the ovigerous period lasts about 28 weeks. Hatching of larvae takes place from January to April, when first zoeae have been found in coastal waters (dos Santos and Peliz 2005). The larval phase includes three zoeal stages whose duration are temperature dependent. Based on laboratory experiments (Figueiredo and Vilela 1972), the estimates of the time that the zoeae take to reach metamorphosis to the megalopa stage range from 15 days (at 17 °C) to 45 days (at 8 °C). Metamorphosis presumably takes place in the plankton, after which the megalopa settles on the bottom.

Despite *Nephrops* adults being one of the most abundant crustacean species inhabiting slope areas, larvae have been comparatively rare in plankton samples collected during 41 oceanographic surveys conducted over a period of 15 years off the Portuguese coast (dos Santos and Peliz 2005). Various factors may contribute to the scarcity of the larvae, from a relatively low fecundity compared with other decapod species to a depressed density of the stocks caused by the fishery. An important factor may also be the slope habitat occupied by the species and the exposure of the Portuguese coast to the open ocean. *Nephrops* larvae are exposed to a huge volume of ocean following hatching, and the interaction between ocean currents in an unbounded ocean with larval behaviour may be a key issue for dispersal, recruitment back to parental populations, and connectivity among high-abundance areas.

The concerns of the present study were to determine to which degree *Nephrops* larvae produced off the south coast of Portugal are transported away from hatching areas and if such transport represents a possible contribution to neighbouring settlement areas. Given the rarity of the larvae in the plankton and the absence of adequate data on their spatial distribution, we used a modelling approach. To this end, a numerical model of the circulation was developed for the south coast of Portugal, to which an individual-based model (IBM) was coupled. The IBM allowed us to simulate the effect of temperature on larvae development rate, as well as incorporate several larval behaviour scenarios.

Models and methods

Ocean model

The simulations were conducted using a free-surface, terrain-following, primitive equation hydrostatic model configurable for fully realistic regional applications. We have used a version of the Regional Ocean Modeling System, ROMS (Shchepetkin and McWilliams 2003, 2005; Wilkin et al. 2005), with embedded nesting capabilities, ROMS-AGRIF (adaptive grid refinement in fortran; Penven et al. 2006). ROMS-AGRIF enables the use of online and offline nesting, thus permitting the regional applications to be built based on basin- and local-scale configurations and to cover a wide range of time and space scales. Examples of ROMS-AGRIF application to western Iberia are reported in Peliz et al. (2007*a*, 2007*b*) and Teles-Machado et al. (2007).

The present configuration was developed based upon the numerical study of Peliz et al. (2007*a*). A summarized description is given here, and for full details about the model configuration, the reader is referred to that paper.

For a realistic simulation of the Gulf of Cadiz and the Southwest Iberian margin, it was necessary to include local and small-scale aspects like the Gibraltar Strait exchange (Mediterranean inflow and outflow) and the wind forcing with sufficient detail to cope with the strong variability in this region. On the other hand, the remote circulation influencing the western limit of the study region (Fig. 1*b*) is as-

Fig. 1. Nested grid configuration used in this study. The bathymetric contours represent the depths of 500 and 1000 m (*a*) and 200 and 800 m (*b*). The spots between the isobath 200 and 800 at (*b*) are the regions with higher catches of *Nephrops norvegicus* adults. The vertical line at longitude 7.5°W indicates the location of the vertical slice shown in Fig. 8. SD, MD, and LD are the small, medium, and large ocean model domains, respectively, and WRF is the atmospheric model domain (i.e., weather research and forecast).

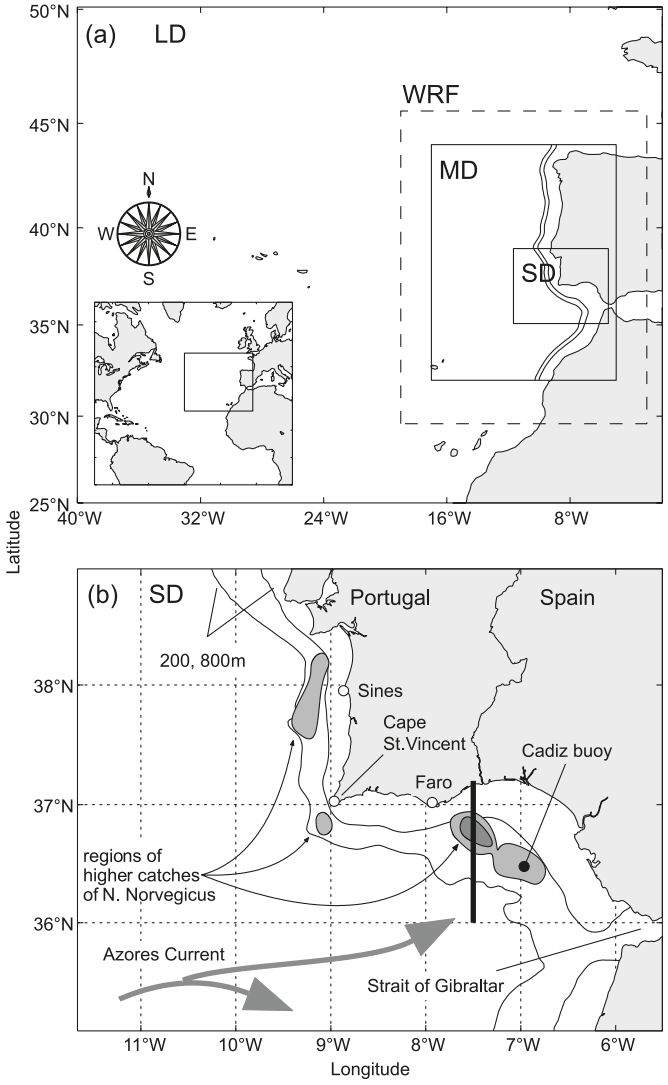

sociated with the Azores Current, which needs to be represented in the model. To resolve the large and small scales, three grids were used (Fig. 1*a*). First, a large domain grid (LD), with resolution around 16 km, between 2°W and 40°W and 25°N to 50°N was used to provide initial fields and lateral boundary conditions to an intermediate domain (MD) with ~9 km resolution (see Fig. 1). In this first step, the communication between LD and MD was done through offline nesting. Secondly, the MD provides information at the model time step (online nesting) to the small ~3 km resolution domain (SD), which constitutes the target domain for the dispersion study, and whose main features are described below.

The LD domain was initialized from rest using monthly temperature and salinity climatological fields (Levitus and Boyer 1994; Levitus et al. 1994) and was forced using monthly surface fluxes from Comprehensive Ocean–Atmosphere Data Set, COADS (da Silva et al. 1994). Along the lateral boundary conditions (south, west, and north), the same climatologies were used for temperature and salinity. Cross-boundary geostrophic velocity plus surface Ekman flow, computed from climatological density and climatological winds, respectively, were also provided on a monthly basis.

This LD configuration was run for 8 years, and equilibrium solutions are reached after 3 years. Although no interannual variability is allowed in the atmosphere nor in the lateral boundary forcing, small differences are observed among the 8 model years. The results from model year 4 LD were used for the initial fields and boundary conditions to the high-resolution-nested simulations (MD with embedded SD). The choice of year 4 for the base experiments is due to the fact that the solution is already in equilibrium, and the temperature and salinity characteristics at the levels of the Mediterranean water mass did not diverge substantially from climatological values, since its representation in the LD configuration is not explicit (a nudging term is used; Peliz et al. (2007*a*)).

In the case of the nested experiments, a realistic Mediterranean undercurrent (MU) was imposed by a boundary inflow and outflow condition at the Strait of Gibraltar (see Peliz et al. 2007*a* for details). This condition induces a slope circulation system that includes the MU and other surface currents (Peliz et al. 2007*a*). The nested experiments were forced with realistic atmospheric model data for the winter period of 2005–2006 (see below), and the ocean–atmospheric fluxes were calculated internally through a bulk flux formulation. The simulations starting date was 1 December 2005, and the experiments were conducted for 4 months. The winter 2005–2006 was characterized by the absence of abnormal atmospheric or oceanographic phenomena and may be considered as a typical winter representative of the present climatic conditions. On the other hand, the interannual variability of larval dispersal is beyond the scope of this study.

To assess the role of ocean internal variability (fluctuations in the current systems not driven by the atmosphere), the nested experiments were also initialized and controlled along the open boundaries with years 3 and 5 LD runs. However, the changes in the slope currents from the different years are small, because the system is largely conditioned by the flow structures associated with the Mediterranean inflow and outflow, which tends to be very stable in nature, and consequently it is kept fixed in the model (see Peliz et al. 2007*a* and references therein). Moreover, in the perspective of the main patterns of larval dispersal, no major differences were observed between the different years, and these experiments are not considered in the analysis below.

Atmospheric model

The global atmospheric reanalysis available for realistic ocean modelling are usually of too low resolution (in the order of 100 km), and the local scale shelf and slope circulation require winds with local detail (Teles-Machado et al. 2007). For that reason, the weather research and forecast

Fig. 2. (*a*) Vertical profile of turbulent diffusivity k and its vertical derivative k', leading to a vertical mixing of the particles through a random process. (*b*) Example of vertical location of a particle in the DVM200 scenario (diel vertical migration between the surface and a depth of 200 m) during 3 days.

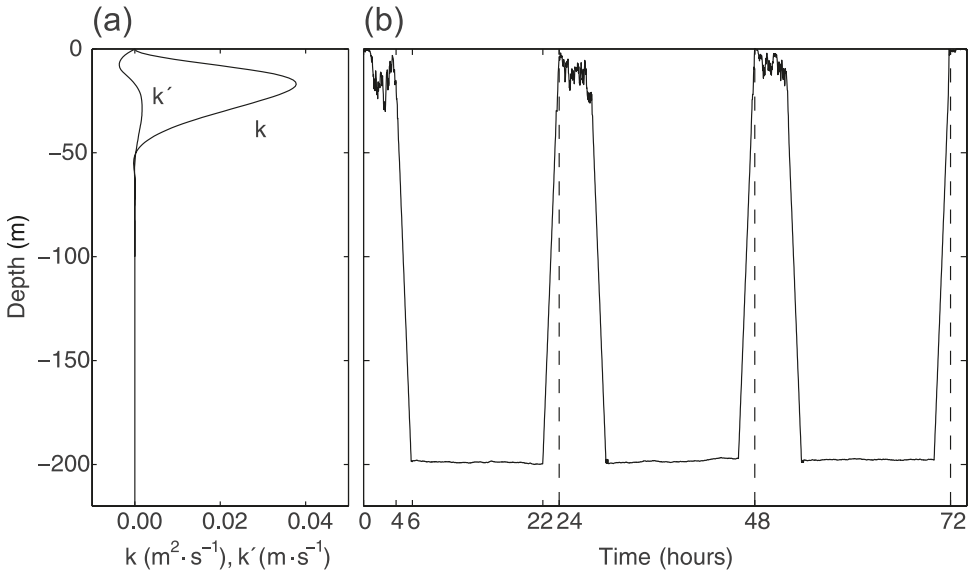

(WRF) atmospheric model was used to dynamically downscale atmospheric reanalysis for the study period. WRF is a widely used research and forecast system (Skamarock et al. 2005), and an application of WRF simulations with ROMS is reported in Teles-Machado et al. (2007). A regional configuration of WRF (see WRF domain in Fig. 1*a*) was set up for the study period from 1 December 2005 to 31 March 2006. The WRF simulations were initialized and forced along the open boundaries with the National Centre for Environment and Prediction reanalysis data (Kalnay et al. 1996). WRF version 2.0 was used with a grid of 15 km and 60 vertical levels. Surface winds, humidity, pressure, temperature, and radiative data were generated and passed to the ocean model to calculate the air sea fluxes. For more details, the reader may refer to Teles-Machado et al. (2007) and Peliz et al. (2007*a*).

IBM

An IBM was coupled to the ROMS-AGRIF model to simulate hatching, development, and behaviour of the larvae. Coupling of the IBM and ROMS-AGRIF was made using a Lagrangian module (Capet et al. 2004; Peliz et al. 2007*b*). At each time step, particles introduced into the model to simulate larvae were advected by the three-dimensional velocity field resulting from the ocean model, with a high-order predictor–corrector time step algorithm. In addition to the advection generated by the model velocities, particle movements included random velocities in the horizontal (controlled by the explicit Lagrangian diffusion) and vertical (controlled by the vertical turbulent diffusivity) direction, which were used to parameterize unresolved turbulent processes. The reader is referred to Peliz et al. (2007*b*) and references therein for a detailed description of the Lagrangian module.

As well as to the advective and diffusive components described above, several behavioural scenarios were imposed on the particles regarding their initial distribution in the water column and their passive or active vertical swimming in an attempt to bracket the uncertainty about the behaviour of *N. norvegicus* larvae. In some of the experiments, a DVM scheme was explicitly introduced to simulate the vertical motion of larvae within the water column depending of the hour of the day. The DVM scheme consisted of forcing the larvae to drift at a deep level (described below) between 0600 and 2200 and at the surface between 0000 and 0400 every day, while during the remaining periods (0400 to 0600 and 2200 to 2400), the larvae migrated vertically from surface to a determined deep level and from that deep level to the surface, respectively (Fig. 2*b*). The scenarios were labelled and defined as follows: U5, passive larvae (no DVM) released uniformly within a 5 m thick surface layer; U50, passive larvae released uniformly between the surface and a depth of 50 m; U200, passive larvae released uniformly between the surface and a depth of 200 m; DVM200, larvae undergoing diel vertical migration between the surface and a depth of 200 m (Fig. 2*b*); DVM400, larvae undergoing diel vertical migration between the surface and a depth of 400 m. We did not include DVM scenarios within the 50 m surface layer. This option was taken because the mixed surface layer is typically deeper than 60 m during winter and because turbulent diffusivity would act as a mixing mechanism overriding the effect of vertical migration on the distribution of the larvae (see Fig. 2*a* for a typical vertical profile of diffusivity (k) and its vertical derivative (k') from which the vertical random displacements are calculated; see Peliz et al. 2007*b*, eq. 5; this effect on depth time series is exemplified in Fig. 2*b*). Because the simulations time started at 0000, larvae from DVM scenarios were released at the surface (DVM larvae are near the surface between 0000 and 0400). The deeper limits of the different scenarios were selected based on whether the larvae prefer surface layers during their development (5 m), considering the chlorophyll maximum layer (50 m) (Moita 2001), the euphotic layer (200 m), and the Mediterranean current upper layer limit

Fig. 3. Temperature-dependent development of laboratory-reared *Nephrops norvegicus* larvae according to Figueiredo (1971) and Figueiredo and Vilela (1972). The figure represents the time to reach the moult to stage IV. A second-order polynomial function was fitted to the centres of the uncertainty intervals, which are represented by the horizontal and vertical bars, and used to calculate development stage by the model.

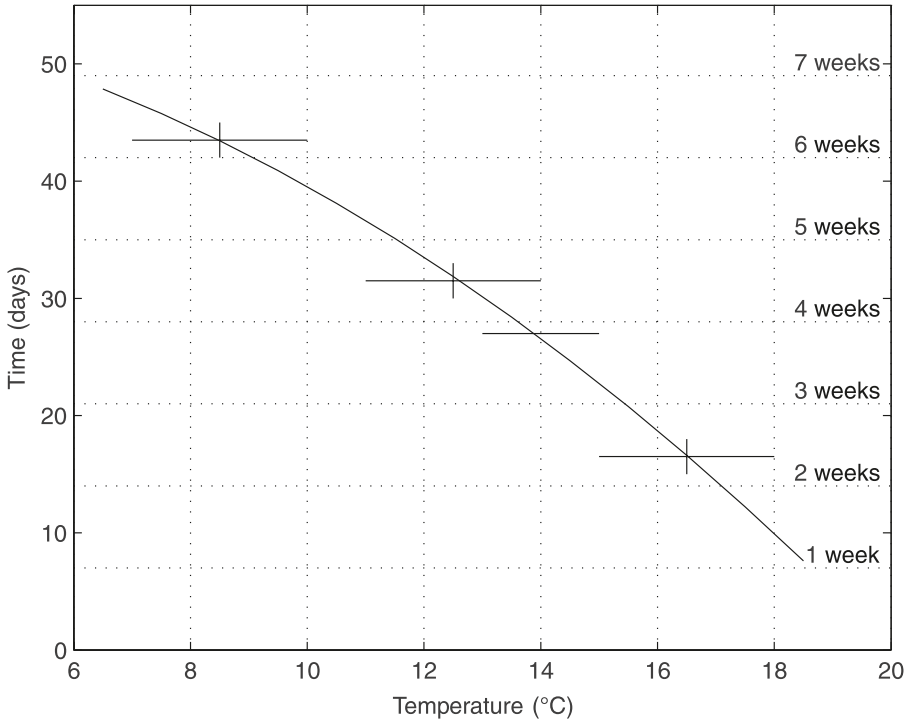

(400 m). Moreover, in the uniform scenarios the larvae were randomly placed from the beginning within the respective depth strata, because a migration from the bottom after hatching would have a negligible effect on horizontal transport.

At 12 to 18 °C, which approximates minimum and maximum temperatures to which larvae may be exposed to during winter in southern Portugal, time to reach the stage of megalopa (stage IV, following the three zoeal stages) varies between 10 and 35 days, respectively (Fig. 3). Relative age of each larva was calculated at each time step of the model, based on the number of minutes a larva is exposed to a specific temperature along its track. The number of degrees × minutes necessary to develop through each stage was estimated from a second-order polynomial fit to the data of temperature-dependent development by Figueiredo (1971) and Figueiredo and Vilela (1972). Relative age was set to 0 at release and 1 at moult to stage IV. Once larvae reached age 1, they were assumed to be competent for settlement and were sent to the bottom and their position was recorded and classified in one of sixteen boxes shown in Fig. 4. The boxes are meridionally or zonally organised and also defined in relation to the 800 m isobath (that roughly delimits the slope zone and the lower limit of distribution of adult *N. norvegicus*). Decapod competent larvae may delay moult to the juvenile stage if an appropriate settling substrate is not available (Rothlisberg 2002). To simulate a possible delay in assuming a benthic life, larvae were allowed to drift along the bottom layer for a period of time arbitrarily set to 1/4 of the time they took to reach age 1. Accordingly, position of the larvae was also recorded at age 1.25.

Five simulation trials were run corresponding to the five behavioural scenarios. The runs started on 1 December 2005 and lasted for 4 months. During the first 2 months of each simulation (December and January), larvae were released every day from a region where the highest densities of spawning lobsters have been historically recorded (e.g., ICES 2006), centred at longitude 7.5°W and latitude 36.8°N (see oval inner dark grey region in Fig. 1*b*, centred at those coordinates). The number of particles released per day followed a Gaussian distribution centred in the middle of the release period (1 January) and with standard deviation of 15 days (Fig. 5). The smallest release was of 227 larvae, corresponding to larvae uniformly separated by a distance of 1.5 km in the region of release. The highest release was 10 times this number during the middle of the release period (Fig. 5). A total number of 83 536 larvae were released per scenario, all from the region defined above.

Results

Ocean and atmosphere model results and comparison with observations

A more systematic validation of the numerical configuration described above, involving comparison with observations and with other studies, is provided in Peliz et al. (2007*a*) and Teles-Machado et al. (2007) (another study (Á. Peliz, P. Marchesiello, A.M.P. Santos, J. Dubert, A. Teles-Machado, M. Marta-Almeida, and B. Le Cann, unpublished data) will present detailed analyses of observations and model currents along the slope zone that include our study period). According to these studies, the current system along

Fig. 4. Division of the studied area (small domain, SD) into 16 boxes where the number of larvae reaching relative ages of 1 and 1.25 was counted. The larvae release location is also shown as the shaded spot centred at 36.8°N, 7.5°W. The 800 m isobath separates the coastal and oceanic boxes.

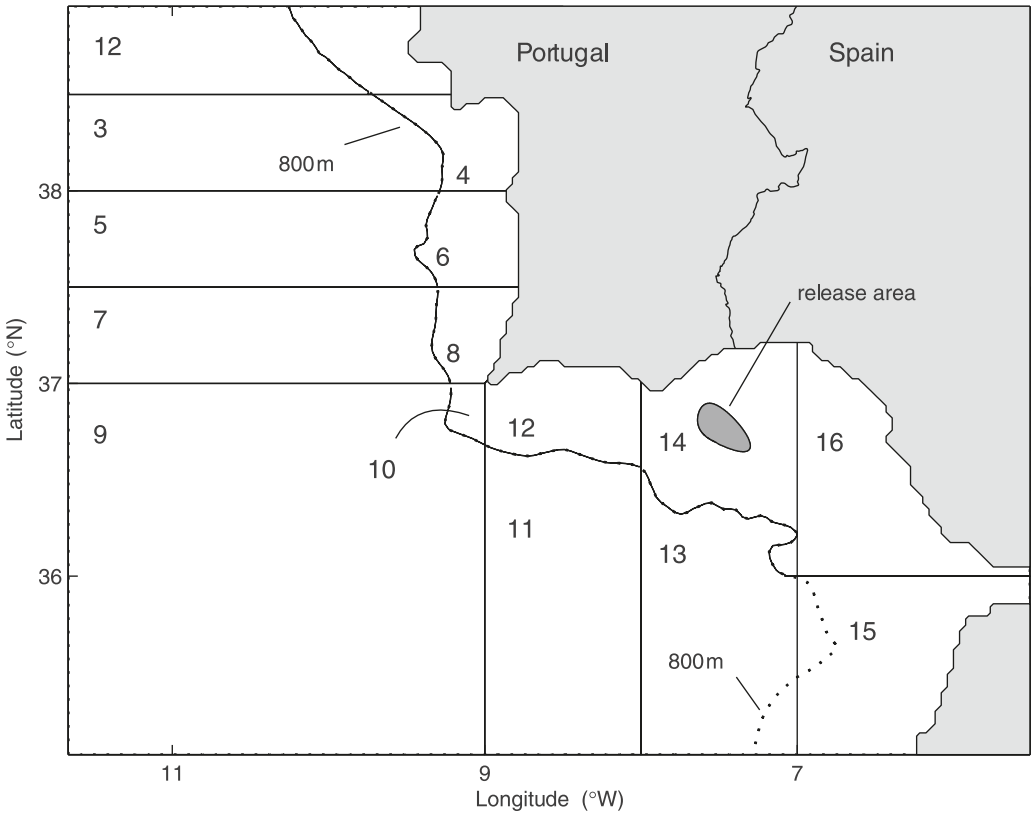

the Gulf of Cadiz slope is largely determined by the dynamics inherent to the coupling between the Mediterranean inflow and outflow, and to a less degree, to the atmospheric forcing. The authors describe a very low correlation between winds and currents at daily to synoptic scales and conclude that the flow variability depends on other factors, hardly controllable in a model simulation, like the internal variability associated with the chaotic nature of the turbulent flow. In this context, a clear match between point observations and corresponding model simulations results is not expectable. Nevertheless, we provide some comparisons of atmosphere and ocean model results with data recorded by an ocean and meteorology surface buoy located at 36.477°N, 6.963°W (denoted by Cadiz buoy, see location at Fig. 1*b*, over the 450 m isobath). This comparison corresponds to the realistic simulation period December 2005 to March 2006.

Observed and simulated wind components are illustrated (*u* and *v* are positive in the east and north directions, respectively) (Fig. 6). Despite the larger variability in the high frequency band of the observations, the model winds represent the major synoptic variability in the observed period, since the match between both wind components is clear. Unfortunately, the available Cadiz buoy record of ocean data only partially overlaps that of the simulation (December 2005 and first week of January 2006). The observed and modelled zonal (*u*, Fig. 7*a*) and meridional (*v*, Fig. 7*b*) surface (3 m) current components are presented. Buoy temperature at 3 m (thick line), satellite-derived sea surface temperature (from Satellite Application Facility (Ocean) (SAFO) database, SAFO (2007)) interpolated at the Cadiz buoy location, and model surface temperature for the same location are illustrated as well (Fig. 7*c*). In what concerns the surface temperature, the model follows the observed values, and the differences are within a range of less than 0.5 °C. The comparison of the model and observed currents shows a fair agreement despite the fact that the observed point is over the slope and relatively far from the shelf. As referred above, the wind-driven component of the currents is reduced, and part of the circulation is due to the internal current variability, which is not predictable, and some of the flow events are not registered or are not in phase in the model and in the observations. For example, the reversals in the north current component by mid-December and beginning of January in the observations time series (Fig. 7*b*) is not in phase with any wind event that could justify such current reversal (Fig. 6). Thus, this reversal in the observed currents is most possibly associated with the meandering and eddy events of the slope system and not with changing wind forcing. This appears to be the reason why in the model simulation these events were not observed in those particular dates. However, they are common in other periods (for a deeper discussion of this subject, see Peliz et al. (2007*a*)).

Main circulation features in the study region

The Gulf of Cadiz constitutes the zone of exchange with the Mediterranean Sea through the Strait of Gibraltar, and

Fig. 5. Number of larvae released per day in each scenario. Larval release followed a Gaussian pattern centred between beginning of December and the end of January, with standard deviation of 1/4 of this period. Total number of larvae released daily varied between 227 and 10 × 227, yielding a total number of 83 536.

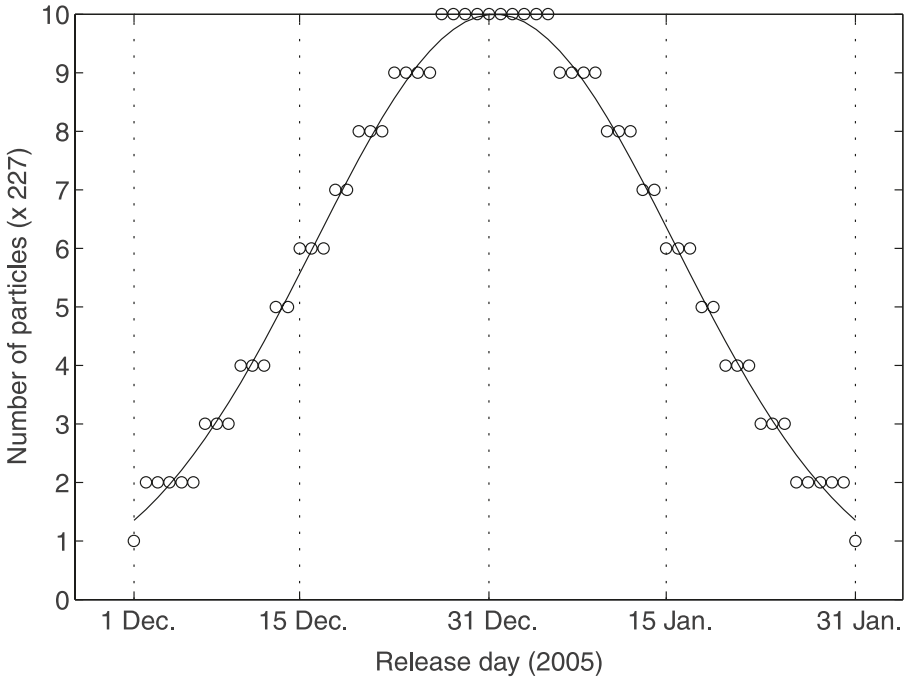

the Mediterranean outflow strongly influences the local circulation, particularly the subsurface flow owing to the presence of the MU. The MU is a bottom-trapped plume of about 100 m thickness, generated by the mixing of Mediterranean outflow waters with the central Atlantic water. The MU is strongly forced by the topography from its generation point until the western part of the Gulf, where the plume reaches a buoyancy equilibrium and starts spreading laterally. Still in the eastern part, the plume splits in two main veins, which after stabilization typically remain centred at depths of 600 to 1200 m, with core velocities in the order of 0.3–0.4 $m \cdot s^{-1}$, transporting warm and salty water from the Mediterranean Basin into the Atlantic Ocean (Baringer and Price 1997; Serra et al. 2005; Peliz et al. 2007*a*).

The model-averaged (December 2005 and January 2006) vertical structure of the alongshore velocity off the southern Portuguese coast, at 7.5°W, is shown (Fig. 8, see the location of the vertical section in Fig. 1*a*; negative (broken lines) and positive (solid lines) values indicate westward or eastward flow, respectively). The MU is present near the bottom and extends to the upper slope, surfacing between 36.6°N and 36.8°N, with westward velocities near 0.1 $m \cdot s^{-1}$ close to the surface.

The complex processes of adjustment of the Mediterranean inflow and outflow are not only important for the bottom currents but also determine the surface and upper slope circulation (Peliz et al. 2007*a*). The MU westward flow is bordered by two eastward (positive) currents (Fig. 8). Offshore, a broad and deep current is driven in association with the mass balance necessary for the entrainment within the MU (a recirculation feature). This flow is observable in the horizontal mean current structure (Fig. 9) as a slope-oriented current with the axis along 36.2°N noticeably east of 8°W and recirculating to the north near the slope where it merges with the MU. Inshore and up-slope of the MU (Fig. 8), a second jet-like feature shallower than 200 m with typical transport of 0.4 Sv (1 Sv = 10^6 $m^3 \cdot s^{-1}$) and velocities of around 0.15 $m \cdot s^{-1}$ is observable. This second equatorward flow is driven by the the inflow of surface Atlantic waters into the Mediterranean Basin, and it is part of a continuous slope equatorward current (denoted by Gulf of Cadiz Current (GCC) in Peliz et al. (2007*a*). The GCC extends from Cape St. Vincent to the Strait of Gibraltar and intensifies east of Faro (see the inshore-most equatorward flow in Fig. 9). Observations of this upper slope current are reported in Garcia-Lafuente et al. (2006) and Garcia Lafuente and Ruiz (2007).

In summary, the circulation in the Gulf of Cadiz is constituted of a bottom-intensified westward flow (the MU) with little but substantial transport at the surface. Offshore, a broad and deep flow is generated in response to the MU, promoting a eastward transport at all depths. Inshore and up-slope of the MU, a second narrow but intense current (the GCC) dominates the upper slope and outer shelf circulation, inducing also a eastward (equatorward) transport. Peliz et al. (2007*a*) (also Á. Peliz, P. Marchesiello, A.M.P. Santos, J. Dubert, A. Teles-Machado, M. Marta-Almeida, and B. Le Cann, unpublished data) thoroughly discuss this circulation scenario and compare it with observations and with other theoretical models. The authors argue that in mean terms, theses circulation features are very persistent and little influenced by the local wind forcing. Thus, they are determinant for transport and dispersal processes with time scales larger that the atmospheric synoptic forcing (a few days to 1 week)

Fig. 6. (*a*) Zonal (*u*) and (*b*) meridional (*v*) components of the wind at the Cadiz "Puertos del Estado" buoy (thin black line) and atmospheric model WRF (i.e., weather research and forecast, thick grey line) for the simulations period. Both represent raw data with samplig rates of 1 h (Cadiz Buoy) and 4 h (WRF).

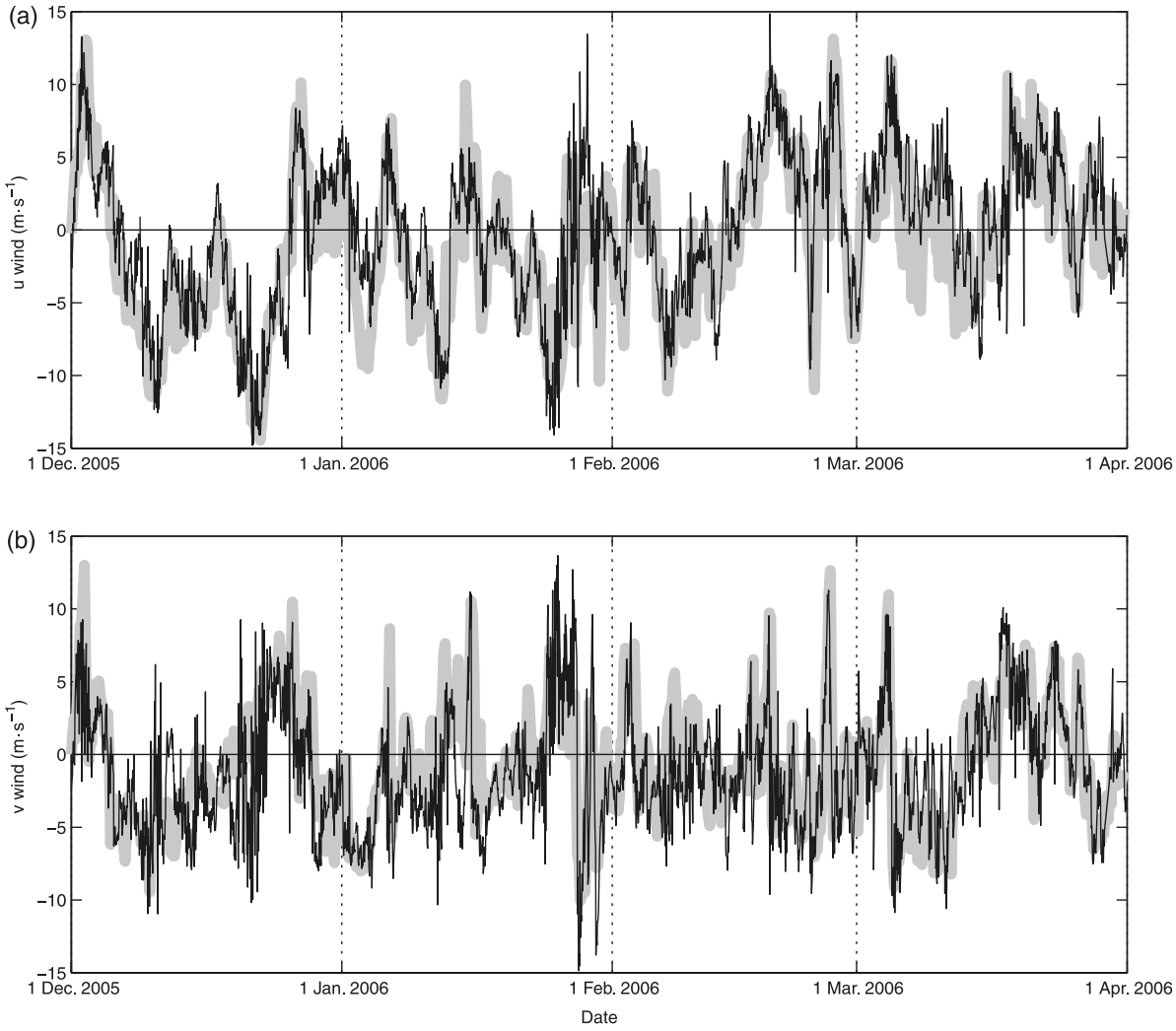

and larger than the typical ocean mesoscale coastal and slope eddy events (several days to 1 or 2 weeks), which match those we are interested in the present study.

General patterns of larval dispersion

The main strategy for the analysis of the IBM results was to register the number of individual particles arriving at given sites after reaching ages 1 and 1.25. This result is interpreted as a proxy for the probability of larvae originating at the release location to settle in that particular area. Since we wished to analyse the actual distribution of settlement over the whole domain, we did not standardize number of larvae per unit area. The number of larvae reaching ages 1 and 1.25 per day (during the simulation period), and arriving at boxes 5 to 16, is illustrated (Fig. 10). Boxes 1 to 4 are not shown because the corresponding values were always zero or very low. The plots are organised into matrices, where the rows refer to boxes and the columns correspond to the five different migration scenarios.

The integrated information for the whole simulation period is shown. For each box, a bar diagram is displayed representing the percentage of larvae that reached age 1 (Fig. 11*a*) and age 1.25 (Fig. 11*b*) in that particular box. Each bar in the diagrams corresponds to the results of a given experiment as has been used for Fig. 10. For example, the sum of the first bar in each diagram corresponds to the 100% of larvae counted inside the 16 boxes. Only a small fraction (less than 5%) of the whole number of larvae abandoned the SD (boxes 1–16) through Gibraltar Strait or the western and southern boundaries.

The majority of larvae reached age 1 or 1.25 along the southern coast inshore of the 800 m isobath (boxes 12, 14, and 16) and in particular in box 14 where larvae were hatched (Fig. 4). This can be seen by summing the percentages given in Fig. 10*b* for boxes 12, 14, and 16 separately for larvae aged 1 and 1.25. These totals ranged from 58.3% to 94.6% in the case of U5, U50, U200, and DVM200 scenarios and were 44.7% and 39.9% in the case of the DVM400 scenario. The only substantial concentrations of larvae offshore of the 800 m isobath were found in the southwest region, mainly in box 9, which corresponds to a larger oceanic area. Another important spatial pattern is that

Fig. 7. (*a*) Zonal (*u*) and (*b*) meridional (*v*) components of surface velocity measured by the Cadiz buoy current meter (thin line) and the surface velocity resulting from the ocean numerical model (thick grey line). (*c*) Comparison of sea surface temperature of model (continuous grey line), buoy (continuous thick line), and Satelite Application Facility (Ocean) (SAFO) database (discontinuous thin line) for the period 1 December 2005 to 6 January 2006. All represent raw data with sampling rates of 1 h (Cadiz buoy), 0.3 h (model data), and 8 h (SAFO temperatures).

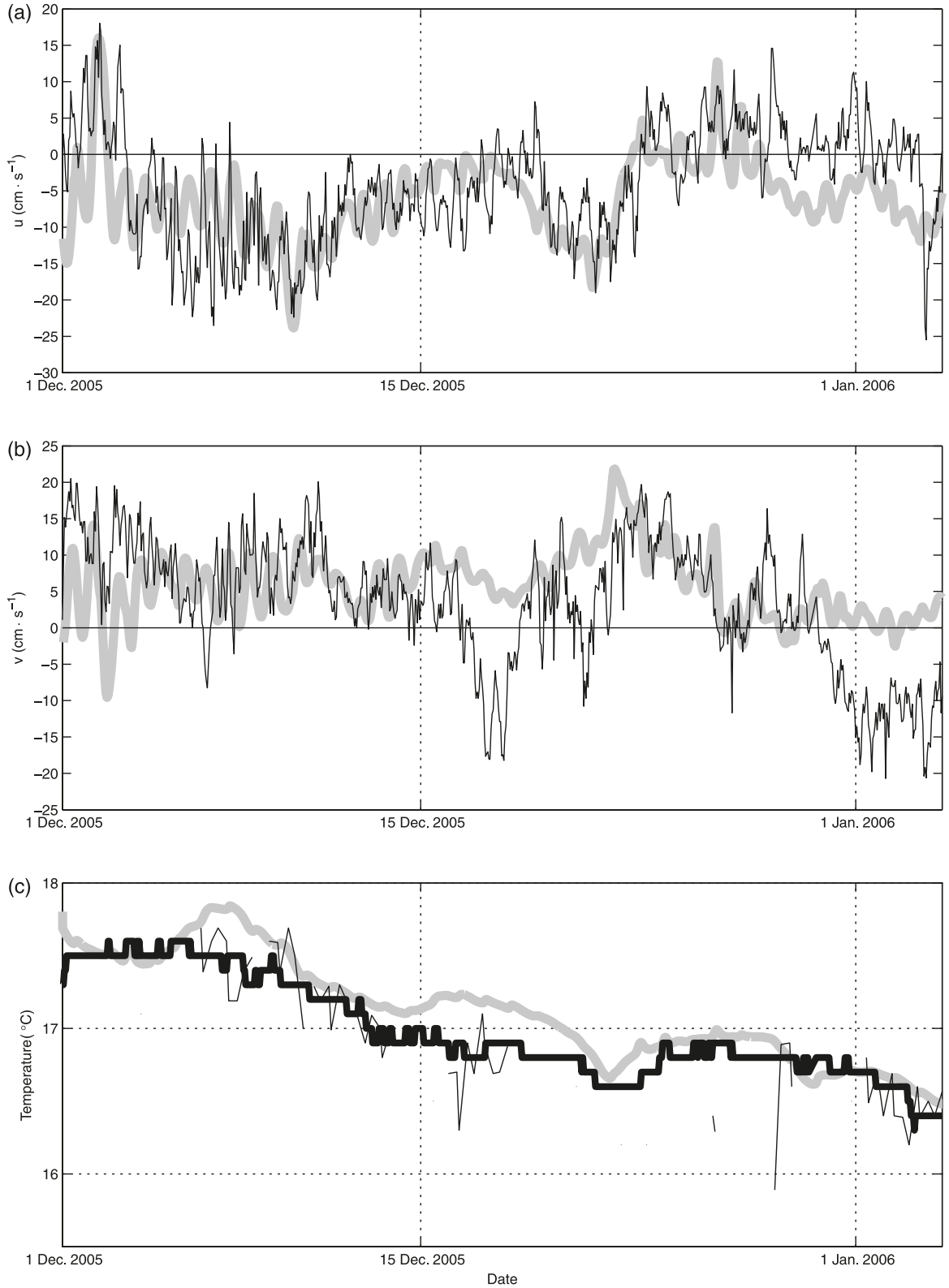

Fig. 8. Mean (December 2005 and January 2006) alongshore velocity at the southern Portuguese coast, at 7.5°W (negative values for broken lines, positive values for solid lines indicate westward or eastward flow, respectively) resulting from the model output. See location of the slice at Fig. 1*b*. MU, Mediterranean undercurrent; GCC, Gulf of Cadiz Current.

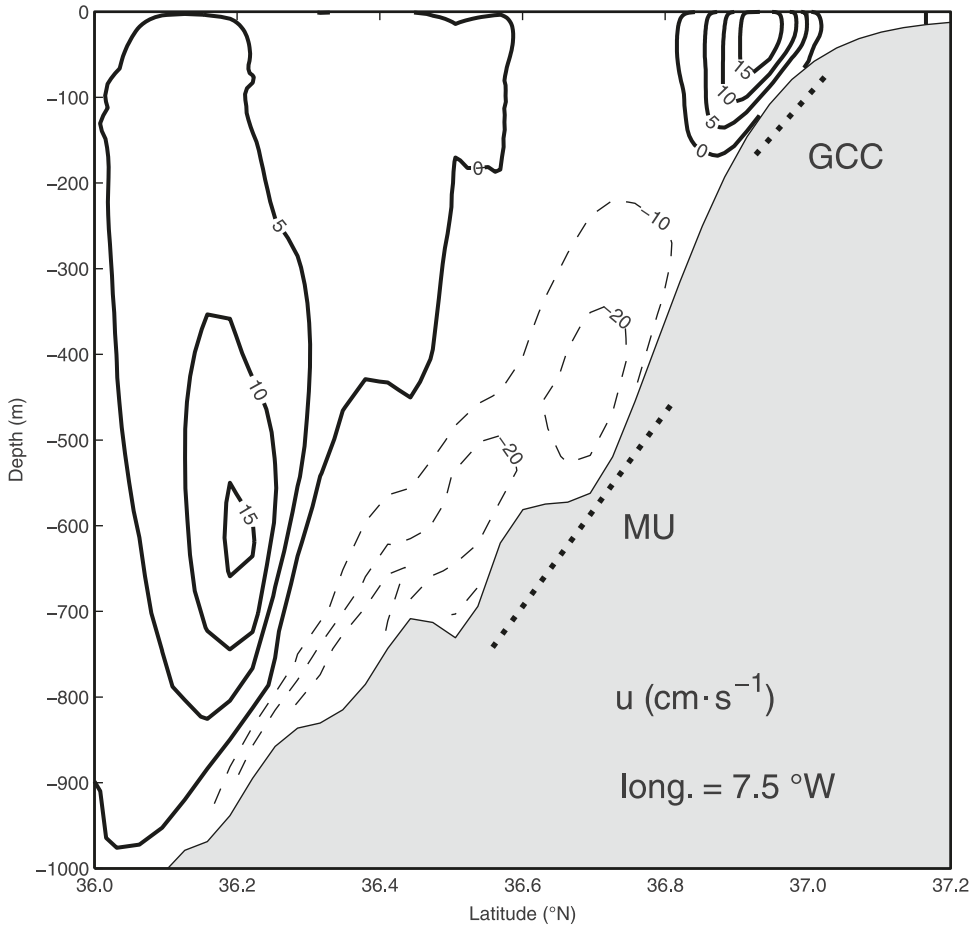

coastal regions off the west coast, north of Cape St. Vincent, received very low numbers of larvae. The sum of percentages in boxes 6 and 8 ranged from 0.0% to 2.2% in the case of uniform and DVM200 scenarios in ages 1 and 1.25 larvae and were 7.5% in the case of the DVM400 scenario for both ages (Fig. 10*a*). North of 38°N (boxes 1 to 4), the number of larvae in the inshore and offshore boxes was very low, typically less than 0.1% of total larvae.

It is worth noting that in spite of box 10 being about two orders of magnitude smaller than box 9 and also smaller than the box adjacent to the east (box 12), the number of larvae that settled there was relatively high, ranging from 0.5% to 6.5% of the larvae released depending on the behavioural scenario and age (Fig. 10*a*). Conversely, the percentage in the area adjacent to the north of box 10 (box 8) was rather low. This suggests box 10 as a passage to western, and to a less extent, northern regions, as verified by analysing the trajectories of the particles (not shown). In boxes 11, 13, and 15, south of Gulf of Cadiz, small numbers of larvae with ages 1 or 1.25 were observed, indicating weak southward larval transport.

Differences between migration scenarios

The most striking difference between uniform and DVM scenarios was observed around the release area (boxes 14, 16). While passive larvae without DVM (i.e., uniform scenarios, U5, U50, and U200) were generally retained or advected eastward toward the Gibraltar Strait, larvae subjected to DVM (DVM200 and DVM400) were dispersed westward and beyond the slope (Fig. 11). In the eastern onshore regions (boxes 14 and 16), an increase of the larval depth range (U5 to DVM400) is associated with a decrease in larvae abundance. In general, the trend for the larvae to stay in deeper layers implied a decrease of larvae in boxes 14 and 16. The opposite behaviour was observed for the western regions, namely boxes 9 and 10 (i.e., the number of larvae increased; Fig. 11). This behaviour is a consequence of the circulation described above, with deep currents of the MU flowing westward (Fig. 8), and the surface GCC flowing in the direction of Gibraltar (Fig. 9).

A bimodal pattern regarding the number of larvae reaching age 1 (but also valid for age 1.25) was observed, mainly in the eastern coastal boxes 14, 16, and to a less extent in box 12), for the uniform scenarios (Fig. 10*b*). The first peak around 10 January originated from the release of particles in relatively warm temperature waters (16.5–17 °C) during the 2 preceding weeks (see Fig. 7*c*). After that period, sea water temperature decreased about 1.3 °C (from 1 January to 1 February). Thus, the time to reach age 1 increased from about 2 weeks (Fig. 3) to about 3 weeks. The second peak

Fig. 9. Mean surface velocities (20 m depth) for the period December 2005 to January 2006 resulting from the model output.

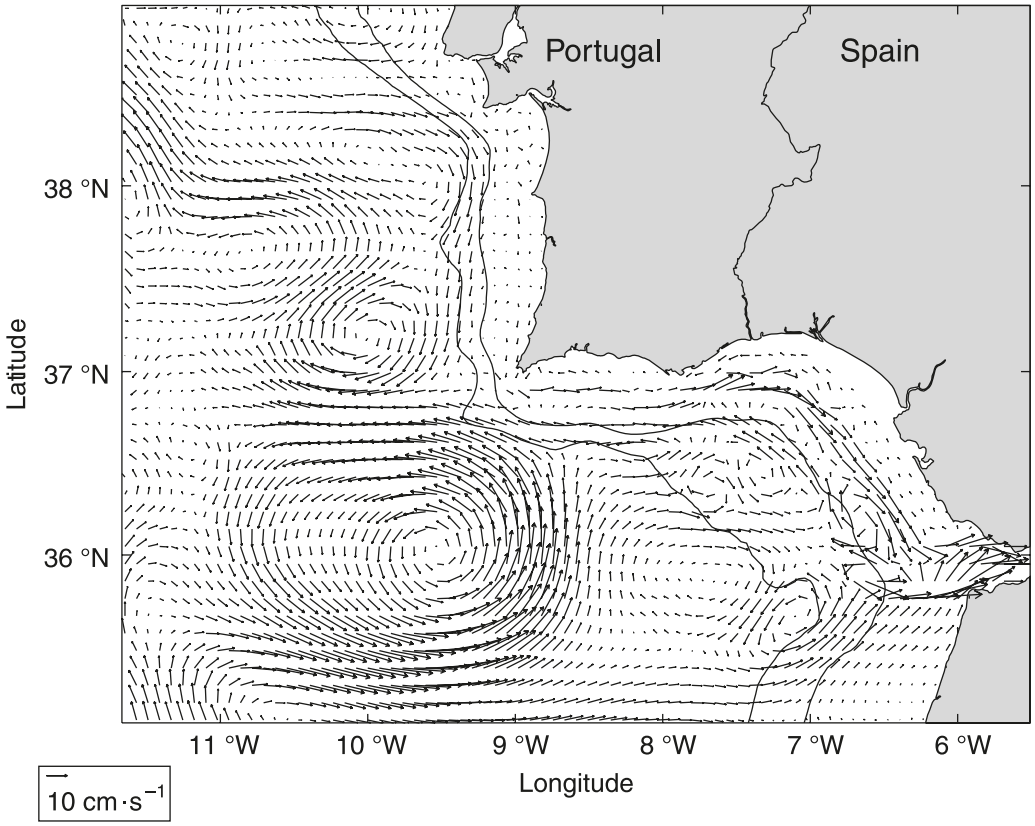

may be explained as the time of response to the maxima of hatched larvae (i.e., corresponds to larvae released around 1 January). For the U200 behavioural scenario, the bimodal peaks were not observed because a relatively large number of larvae were isolated from the surface. Note that below the surface mixed layer, the temperature is nearly constant in time. Thus, in scenarios DVM200 and DVM400, the same behaviour as U200 was observed.

Another important difference between the uniform and DVM scenarios concerns the exchange of larvae to regions north of 37°N. While DVM400 larvae were found in relatively high numbers in boxes 5, 6, 7, and 8, larvae behaving according to uniform scenarios were almost always absent in these areas (with the exception of U200). This can be easily observed in the spatial distribution of larvae by 1 February, 1 month after the release maxima (Figs. 12*a* and 12*c*).

Comparison of ages 1 and 1.25

The time series of the number of larvae becoming adult show a displacement of about 1 week between the time to reach ages 1 and 1.25 (Fig. 10). This is not a surprising result because 0.25 units of age represent about 1 week for a temperature of 14 °C (Fig. 3). At age 1.25 (Fig. 11*b*), since the larvae from all behavioural scenarios are forced to remain in the bottom layer from age 1, they are expected to predominantly move in the westward direction. For instance, in boxes 9 and 10 the number of larvae is strongly increased for uniform scenarios at age 1.25 (Fig. 11). In box 9 the increase is from less than 1% to about 14% in scenarios U5 and U50. As result, there was a decrease in larvae that reached age 1.25 in the onshore regions of the south coast in all scenarios, relative to age 1 larvae. This again can be seen by summing the percentage of larvae reaching ages 1 and 1.25 in boxes 12, 14, and 16 (Fig. 10*b*). While in the case of age 1.25 larvae the values ranged from 39.9% to 79.2%, they ranged from 44.7% to 94.6% in the case of age 1 larvae. This behaviour is due to the advection of larvae by the MU, and larvae are exported (and lost) to the open ocean (box 9). The spatial distribution of larvae with ages 1 and 1.25 by 1 February (Fig. 12) is representative of the general patterns of larval dispersal. For uniform scenarios in Figs. 12*a* and 12*b*, the comparison of age 1 with age 1.25 indicates a clear westward transport due to MU. For DVM scenarios in Figs. 12*c* and 12*d*, such a clear difference between ages is not observed because the larvae are influenced by the MU during the entire life history.

Discussion

The spatial patterns of distribution of competent larvae predicted by the simulations can be explained by the circulation features off the south coast of Portugal. While the deeper layers are dominated by the westward-flowing MU (Ambar and Howe 1979), near the surface the GCC (Peliz et al. 2007*a*) flows eastward over the upper slope towards the Strait of Gibraltar. Moreover, circulation over the shelf areas shoreward of the main core of the GCC is directly controlled by the meridional component of the wind, which shows periods of 10–15 days dominated by negative or positive values, resulting in currents flowing alternately westward and eastward. The interaction of the MU and

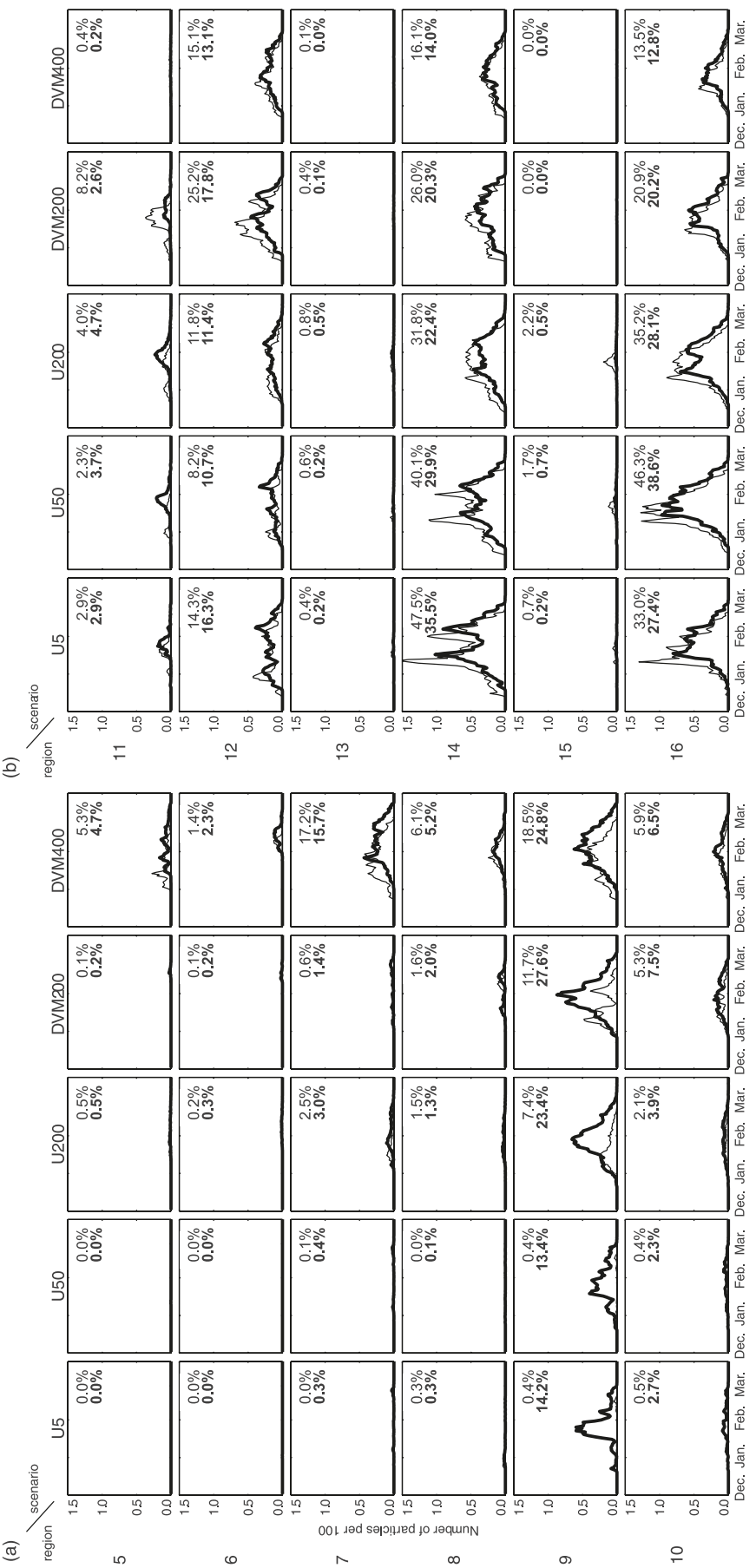

Fig. 10. Number of larvae reaching relative ages of 1 and 1.25 in boxes 5 to 10 (*a*) and 11 to 16 (*b*). Each row of plots represents one box, and the columns represent the behavioural scenarios. The thin line in each plot is the time series of larvae at age 1, starting at the beginning of the simulation period (1 December 2005). The light-font number represents the percentage of the total larvae released that reached age 1 in the corresponding box. Bold lines and numbers represent the same for larvae at age 1.25.

Fig. 11. Percentage of total larvae reaching relative ages of 1 (*a*) and 1.25 (*b*) in each of the 16 boxes. The groups of five bars represent the five behavioural scenarios (from left to right): U5, passive larvae (no diel vertical migration (DVM)) released uniformly within a 5 m thick surface layer; U50, passive larvae released uniformly between the surface and a depth of 50 m; U200, passive larvae released uniformly between the surface and a depth of 200 m; DVM200, larvae undergoing diel vertical migration between the surface and a depth of 200 m; DVM400, larvae undergoing diel vertical migration between the surface and a depth of 400 m.

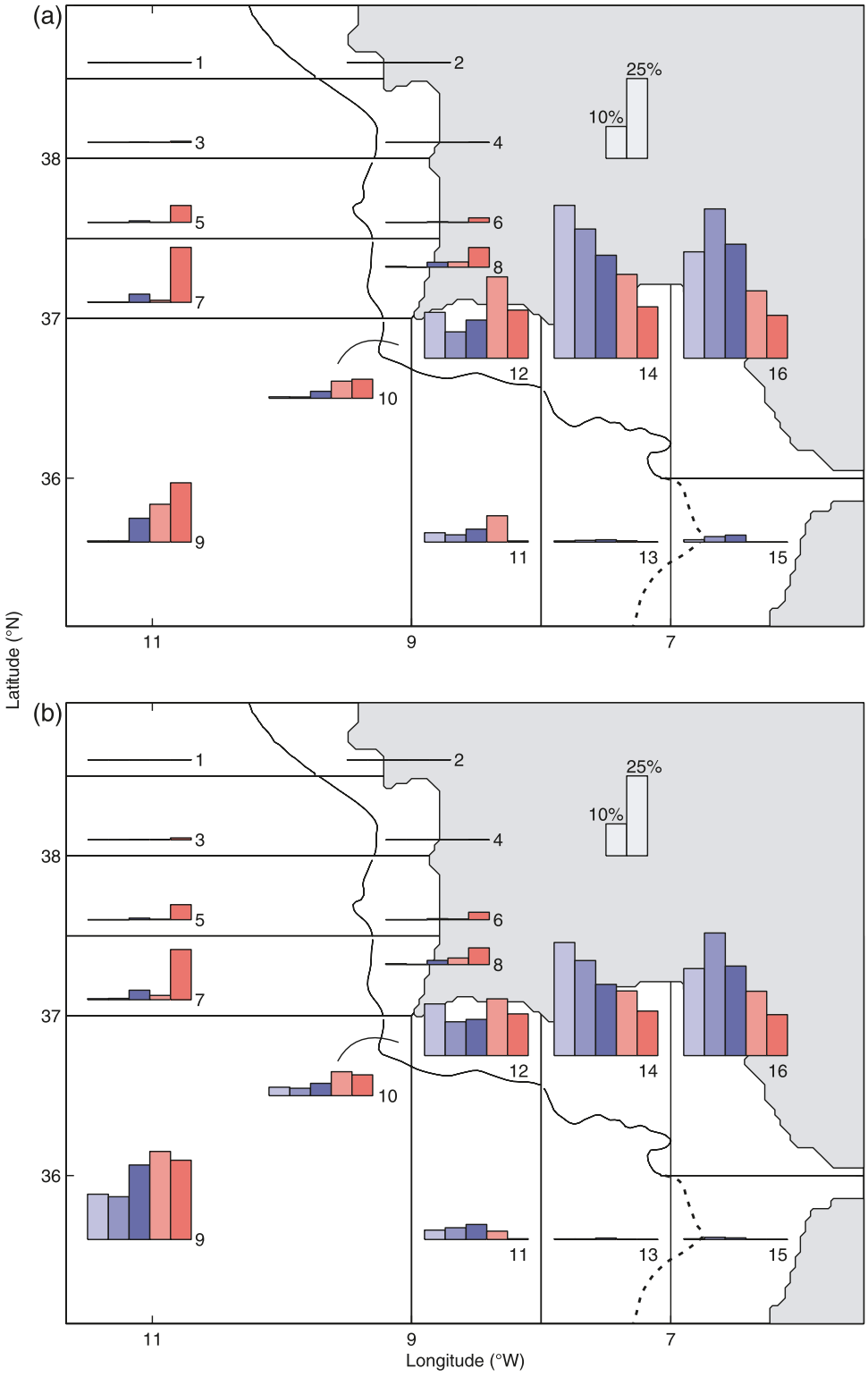

Fig. 12. Spatial larval distribution on 1 February for the scenarios U5 (passive larvae (no diel vertical migration (DVM)) released uniformly within a 5 m thick surface layer; top row) and DVM400 (larvae undergoing diel vertical migration between the surface and a depth of 400 m; bottom row). Panels *a* and *c* refer to age 1; panels *b* and *d* refer to age 1.25.

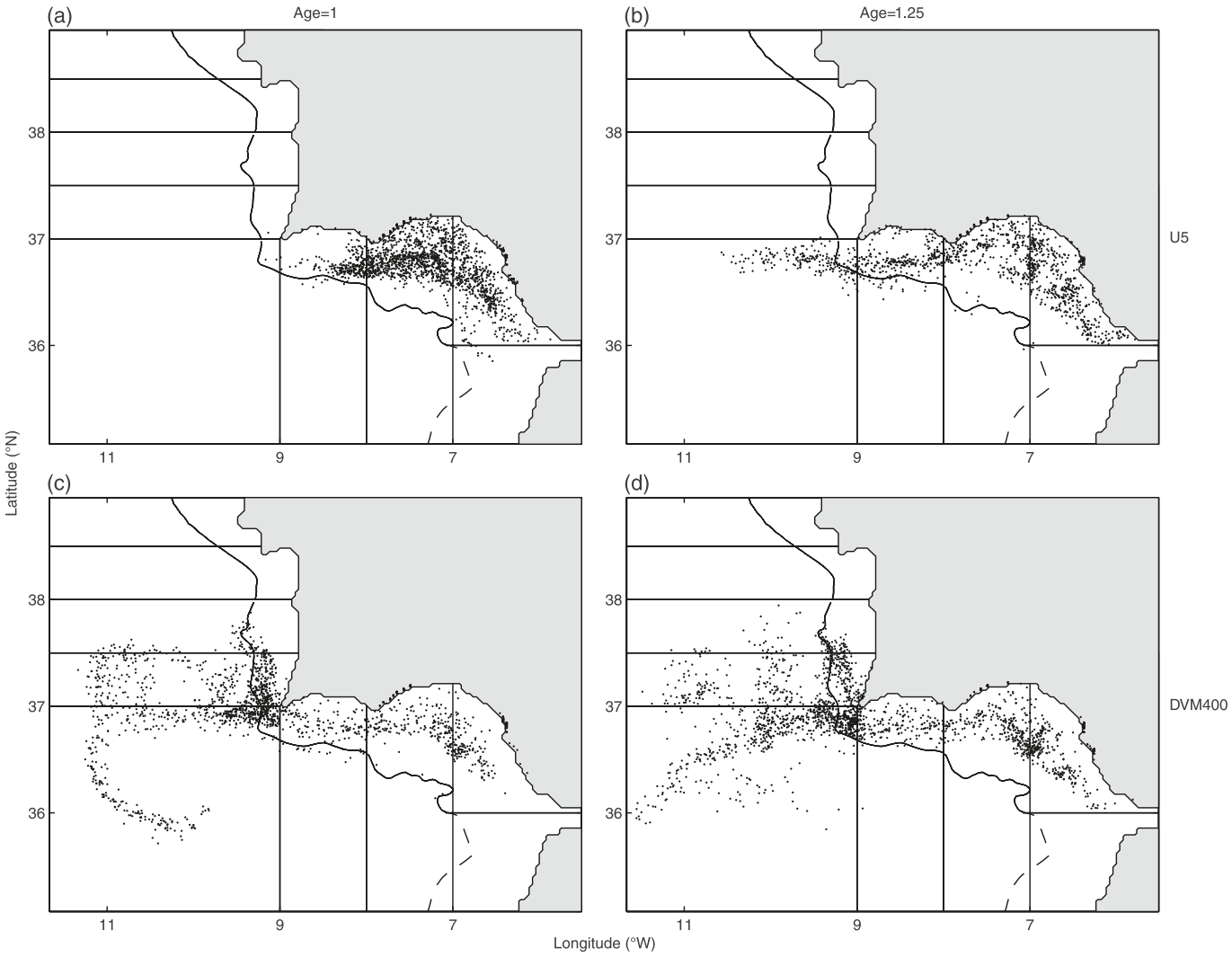

GCC flows with the coastal topography, the bathymetry, and with each other results in pairs of cyclonic and anticyclonic eddies. These eddies are transient structures but tend to be recurrent at the same locations, leaving a strong signature on the mean circulation (Peliz et al. 2007*a*). The most important pair is located to the west and south-southwest of Cape St. Vincent, but smaller structures are also present in the Gulf of Cadiz. Accordingly, the retention of the larvae in the onshore regions of the south coast, where the largest densities of adults are found, can be interpreted as resulting from the interaction of the GCC with the coastal wind-driven circulation, and the probability of retention in this general area increases, as the behavioural scenarios predict a shallower distribution of the larvae. Larvae transported to the central Gulf of Cadiz (boxes 11, 13, and 15) and to the offshore areas of the west coast (boxes 5, 7, and 9) will be trapped by the gyres or channelled offshore and lost from the system. The possibility remains that some of the larvae can be transported to the coastal areas of the west coast and settle there. The simulations show that very few larvae remaining in the upper 50 m will be transported there, but that a deeper distribution increases the probability of northward transport around Cape St. Vincent.

The values presented above for the percentage of larvae advected to the different regions allow an assessment of the general patterns of *N. norvegicus* larval dispersal in the area. These values do not include the effect of larval mortality. Mortality values currently reported in the literature for invertebrate larvae range from 0.02 to 0.82 per day (Morgan 1995). These values were generally obtained by following a cohort of larvae through space and recording self-thinning or by integrating abundances of successive stages over a given area. In both cases, these values apply to mortality during the planktonic life and, as such, do not include mortality from failing to find an appropriate settlement substrate or habitat. Additionally, both methods do not consider the distribution of mortality factors over the large geographical span of many populations, and the integration method does not usually account for losses due to advection from the area (Helbig and Pepin 1998). Nevertheless, the current consensus is that the majority of larvae, in many cases more than 90%, will die before starting the search for an appropri-

ate substrate to settle. Thus, the combined effects of mortality due to disease, starvation, predation, and wastage from appropriate habitats has a decisive effect on the dynamics of marine populations (Gaines and Lafferty 1995; Caley et al. 1996; Morgan 2001). A tentative estimate of the proportion of *N. norvegicus* larvae hatched from the area of high density of adults that self-recruit into that same area can be obtained by (*i*) calculating the number of larvae that settle in that area and (*ii*) using a survival estimate of 0.15 (from hatching to stage III for larvae in the Irish Sea) (figure 9 and table 5 in Dickey-Collas et al. 2000), which is a conservative value given that it does not account for mortality during stage III. Scenarios U50 and DVM400 were those that resulted in the largest and smallest self-recruitment, with values of 3.2% and 1.0%, respectively. Applying a survival estimate of 0.15 to the case of age 1 larvae under these extreme scenarios indicates that only 0.5%, if they remain in surface waters, to 0.2%, if they migrate between the surface and 400 m, of the larvae hatched would successfully self-recruit.

Generalizations of this level of recruitment to the whole region covered by the Algarve stock must be made with caution because this estimate does not consider possible subsidies form neighbouring populations, which are not necessarily identical in their capacity to act as sources or sinks of larvae (Fogarty 1988; Armworth 2002). Nevertheless, these estimates highlight the potential for dispersal of *N. norvegicus* larvae away from the hatching sites in the environmental setting of southern Portugal and show that a considerable proportion may be lost to deeper areas of the open ocean where settlement success is very unlikely. The results of the simulations also show that an important proportion of larvae hatched from the Algarve stock may recruit into the small stock off Cape St. Vincent and that a smaller fraction may reach the stock on the west coast off Sines. Whether these contributions of the Algarve stock in terms of self-recruitment and recruitment subsidies to other local populations have any demographic meaning, in the sense that they are enough to compensate for local mortality (Cowen et al. 2006), cannot be answered by the present study. However, it appears that transport of *N. norvegicus* larvae over distances of 100–300 km along the south and southwest Atlantic coasts of the Iberian Peninsula is possible and that these populations may be genetically connected.

Acknowledgements

This work was funded by the Fundação para a Ciência e a Tecnologia (FCT) through the research contracts LobAssess (POCTI/BIA-BDE/59426/2004) and Clibeco (POCI/CLI/57752/2004). Wind data and surface currents provided by Puertos del Estado (Spain) are gratefully acknowledged. Financial support was allocated by FCT under the Support Community Framework III, Operational Programme Science, Technology and Innovation.

References

Ambar, I., and Howe, M.R. 1979. Observations of the Mediterranean outflow: I. mixing in the Mediterranean outflow. Deep-Sea Res. Part A Oceanogr. Res. Pap. **26**: 535–554. doi:10.1016/0198-0149(79)90095-5.

Armworth, P.R. 2002. Recruitment limitation, population regulation, and larval connectivity in reef fish metapopulations. Ecology, **83**: 1092–1104.

Bailey, N., Chapman, C.J., Afonso-Dias, M., and Turrell, W. 1995. The influence of hydrographic factors on *Nephrops* distribution and biology. ICES-CM Q:17.

Baringer, M., and Price, J. 1997. Mixing and spreading of the Mediterranean outflow. J. Phys. Oceanogr. **27**: 1654–1677. doi:10.1175/1520-0485(1997)027<1654:MASOTM>2.0.CO;2.

Caley, M.J., Carr, M.H., Hixon, M.A., Hughes, T.P., Jones, G.P., and Menge, B.A. 1996. Recruitment and the local dynamics of open marine populations. Annu. Rev. Ecol. Syst. **27**: 477–500. doi:10.1146/annurev.ecolsys.27.1.477.

Capet, X.J., Marchesiello, P., and McWilliams, J.C. 2004. Upwelling response to coastal wind profiles.. Geophys. Res. Lett. **31**: L13311. doi:10.1029/2004GL020123.

Cowen, R.K., Paris, C.B., and Srinivasan, A. 2006. Scaling of connectivity in marine populations. Science (Washington, D.C.), **311**: 522–527. doi:10.1126/science.1122039. PMID:16357224.

da Silva, A., Young, A.C., and Levitus, S. 1994. Atlas of surface marine data 1994. Vol. 1. Algorithms and procedures. NOAA Atlas NESDIS 6. US Department of Commerce, Washington, D.C.

Dickey-Collas, M., Briggs, R.P., Armstrong, M.J., and Milligan, S.P. 2000. Production of *Nephrops norvegicus* larvae in the Irish Sea. Mar. Biol. (Berl.), **137**: 973–981. doi:10.1007/s002270000404.

dos Santos, A., and Peliz, A. 2005. The occurrence of Norway lobster (*Nephrops norvegicus*) larvae off the Portuguese coast. J. Mar. Biol. Assoc. U. K. **85**: 937–941. doi:10.1017/S0025315405011914.

Farmer, A.S.D. 1974. Reproduction in *Nephrops–Norvegicus* (Decapoda: Nephropidae). J. Zool. **174**: 161–183.

Figueiredo, M.J. 1971. Sobre a cultura de crustáceos decápodes em laboratório: *Nephrops norvegicus* (lagostim) e *Penaeus kerathurus* (camarão). Bol. Inform. Inst. Biol. Marít. **1**: 1–17.

Figueiredo, M.J., and Thomas, H.J. 1967. On the biology of the Norway Lobster, *Nephrops norvegicus* (L.). ICES J. Mar. Sci. **31**: 89–101. doi:10.1093/icesjms/31.1.89.

Figueiredo, M.J., and Vilela, M.H. 1972. On the artificial culture of *Nephrops norvegicus* reared from the egg. Aquaculture, **1**: 173–180. doi:10.1016/0044-8486(72)90017-8.

Fogarty, M. 1988. Implications of migration and larval interchange in American lobster (*Homarus americanus*) stocks: spatial structure and resilience. *In* Proceedings of the North Pacific Symposium on Invertebrate Stock Assessment and Management, 6–10 March 1995, Nanaimo, B.C. *Edited by* G.S. Jamieson and A. Campbell. Vol. 125. Can. Spec. Publ. Fish. Aquat. Sci. pp. 273–283.

Gaines, S.D., and Lafferty, K.D. 1995. Modelling the dynamics of marine species: the importance of incorporating larval dispersal. *In* Ecology of marine invertebrate larvae. *Edited by* L. McEdward. CRC Press, New York. pp. 389–412.

Garcia Lafuente, J., and Ruiz, J. 2007. The Gulf of Cádiz pelagic ecosystem: a review. Prog. Oceanogr. **74**: 228–251. doi:10.1016/j.pocean.2007.04.001.

Garcia-Lafuente, J., Delgado, J., Criado-Aldeanueva, F., Bruno, M., del Rio, J., and Miguel Vargas, J. 2006. Water mass circulation on the continental shelf of the Gulf of Cádiz. Deep-Sea Res. II Top. Stud. Oceanogr. **53**: 1182–1197. doi:10.1016/j.dsr2.2006.04.011.

Harding, D., and Nichols, J.H. 1987. Plankton surveys off the north-east coast of England in 1976: an introductory report and summary of the results. Ministry of Agriculture, Directorate of Fisheries Research, Lowestoft, UK. Fish. Res. Tech. Rep. 86.

Helbig, J.A., and Pepin, P. 1998. Partitioning the influence of physical processes on the estimation of ichthyoplankton mortality rates. I. Theory. Can. J. Fish. Aquat. Sci. **55**: 2189–2205. doi:10.1139/cjfas-55-10-2189.

Hill, A.E. 1990. Pelagic dispersal of Norway lobster *Nephrops norvegicus* larvae examined using an advection–diffusion–mortality model. Mar. Ecol. Prog. Ser. **64**: 217–226. doi:10.3354/meps064217.

Hillis, J.P. 1974. Field observations of larvae of the Dublin Bay prawn *Nephrops norvegicus* (L.) in the western Irish Sea. Ir. Fish. Investig. Ser. B (Mar.), **13**: 1–24.

ICES. 2006. Report of the Working Group on the Assessment of Southern Shelf Stocks of Hake, Monk and Megrim (WGHMM). ICES CM 2006/ACFM 29.

Kalnay, E., Kanamitsu, M., Kistler, R., Collins, W., Deaven, D., Gandin, L., Iredell, M., Saha, S., White, G., Woollen, J., Zhu, Y., Leetmaa, A., Reynolds, R., Chelliah, M., Ebisuzaki, W., Higgins, W., Janowiak, J., Mo, K., Ropelewski, C., Wang, J., Jenne, R., and Joseph, D. 1996. The NCEP/NCAR 40-year reanalysis project. Bull. Am. Meteorol. Soc. **77**: 437–471. doi:10.1175/1520-0477(1996)077<0437:TNYRP>2.0.CO;2.

Levitus, S., and Boyer, T.P. 1994. World ocean atlas 1994. Vol. 4. Temperature. NOAA Atlas NESDIS 4. US Department of Commerce, Washington, D.C.

Levitus, S., Burgett, R., and Boyer, T.P. 1994. World ocean atlas 1994. Vol. 3. Salinity. NOAA Atlas NESDIS 3. US Department of Commerce, Washington, D.C.

Lindley, J.A., Williams, R., and Conway, D.V.P. 1994. Variability in dry weight and vertical distributions of decapod larvae in the Irish Sea and North Sea during the spring. Mar. Biol. (Berl.), **120**: 385–395. doi:10.1007/BF00680212.

Maltagliati, F., Camilli, L., Biagi, F., and Abbiati, M. 1998. Genetic structure of Norway lobster, *Nephrops norvegicus* (L.) (Crustacea: Nephropidae), from the Mediterranean Sea. Sci. Mar. **62**: 91–99.

Maynou, F.X., Sardá, F., and Conan, G.Y. 1998. Assessment of the spatial structure and biomass evaluation of *Nephrops norvegicus* (L.) populations in the northwestern mediterranean by geostatistics. ICES J. Mar. Sci. **55**: 102–120. doi:10.1006/jmsc.1997.0236.

Moita, M.T. 2001. Estrutura, variabilidade e dinâmica do fitoplâncton na costa de Portugal continental. [Structure, variability, and dynamics of phytoplankton in the Portuguese Mainland coast.] Ph.D. thesis, University of Lisbon, Portugal.

Morgan, S.G. 1995. Life and death in the plankton: larval mortality and adaptation. *In* Ecology of marine invertebrate larvae. Chapter 9. *Edited by* L. McEdward. CRC Press, Boca Raton, Fla. pp. 279–321.

Morgan, S.G. 2001. The larval ecology of marine communities. *In* Marine community ecology. *Edited by* M.D. Bertness, S.D. Gaines, and M.E. Hay. Sinauer Associates, New York. pp. 159–182.

Peliz, A., Dubert, J., Marchesiello, P., and Teles-Machado, A. 2007*a*. Surface circulation in the Gulf of Cádiz: model and mean flow structure. J. Geophys. Res. **112**: C11015. doi:10.1029/2007JC004159.

Peliz, A., Marchesiello, P., Dubert, J., Roy, P., Marta-Almeida, M., and Queiroga, H. 2007*b*. A study of crab larvae dispersal off western Iberia: physical processes. J. Mar. Syst. **68**: 215–236. doi:10.1016/j.jmarsys.2006.11.007.

Penven, P., Debreu, L., Marchesiello, P., and McWilliams, J.C. 2006. Evaluation and application of the ROMS 1-way embedding procedure to the central California upwelling system. Ocean Model. **12**: 157–187. doi:10.1016/j.ocemod.2005.05.002.

Queiroga, H., and Blanton, J. 2004. Interactions between behavior and physical forcing in the control of horizontal transport of decapod crustacean larvae. Adv. Mar. Biol. **47**: 107–214. doi:10.1016/S0065-2881(04)47002-3. PMID:15596167.

Rothlisberg, P.C. 2002. The biology of decapod crustacean larvae *Crustacean Issues* volume 14 — Klaus Anger. [Book review.] J. Exp. Mar. Biol. Ecol. **279**: 89–90. doi:10.1016/S0022-0981(02)00381-7.

SAFO. 2007. Satelite Application Facility (Ocean). Available from www.ifremer.fr/cersat [accessed July 2006].

Serra, N., Ambar, I., and Käse, R. 2005. Observations and numerical modelling of the Mediterranean outflow splitting and eddy generation. Deep-Sea Res. Part II Top. Stud. Oceanogr. **52**: 383–408. doi:10.1016/j.dsr2.2004.05.025.

Shchepetkin, A.F., and McWilliams, J.C. 2003. A method for computing horizontal pressure-gradient force in an oceanic model with a nonaligned vertical coordinate. J. Geophys. Res. **108**(C3): 3090. doi:10.1029/2001JC001047.

Shchepetkin, A.F., and McWilliams, J.C. 2005. The Regional Ocean Modeling System (ROMS): a split-explicit, free-surface, topography-following-coordinates oceanic model. Ocean Model. **9**: 347–404. doi:10.1016/j.ocemod.2004.08.002.

Skamarock, W.C., Klemp, J.B., Dudhia, J., Gill, D.O., and Barker, D.M. Wang,W., Powers, J. G., 2005. A description of the advanced research WRF Version 2. Tech. Rep. MMMD-NCAR, Boulder, Colo.

Stamatis, C., Triantafyllidis, A., Moutou, K.A., and Mamuris, Z. 2004. Mitochondrial DNA variation in Northeast Atlantic and Mediterranean populations of Norway lobster, *Nephrops norvegicus*. Mol. Ecol. **13**: 1377–1390. doi:10.1111/j.1365-294X.2004.02165.x. PMID:15140084.

Stamatis, C., Triantafyllidis, A., Moutou, K.A., and Mamuris, Z. 2006. Allozymic variation in Northeast Atlantic and Mediterranean populations of Norway lobster, *Nephrops norvegicus*. ICES J. Mar. Sci. **63**: 875–882. doi:10.1016/j.icesjms.2006.01.006.

Teles-Machado, A., Peliz, A., Dubert, J., and Sanchez, R. 2007. On the onset of the Gulf of Cadiz Coastal Contercurrent. Geophys. Res. Lett. **34**: L12601. doi:10.1029/2007GL030091.

Tuck, I.D., Atkinson, R.J.A., and Chapman, C.J. 2000. Population biology of the Norway lobster, *Nephrops norvegicus* (L.) in the Firth of Clyde, Scotland II: fecundity and size at onset of sexual maturity. ICES J. Mar. Sci. **57**: 1227–1239. doi:10.1006/jmsc.2000.0809.

White, R.G., Hill, A.E., and Jones, D.A. 1988. Distribution of *Nephrops norvegicus* (L.) larvae in the western Irish Sea: an example of advective control on recruitment. J. Plankton Res. **10**: 735–747. doi:10.1093/plankt/10.4.735.

Wilkin, J.L., Arango, H., Haidvogel, D.B., Lichtenwalner, C.S., Glenn, S.M., and Hedström, K.S. 2005. A regional ocean modeling system for the long-term ecosystem observatory. J. Geophys. Res. **110**: C06S91. doi:10.1029/2003JC002218.